Poly(etherimide)/Montmorillonite Nanocomposites Prepared by Melt Intercalation

Zhu-Mei Liang, Jie Yin

Research Institute of Polymer Materials, School of Chemistry and Chemical Technology, State Key Lab of Composite Materials, Shanghai Jiao Tong University, Shanghai 200240, China

Received 28 October 2002; accepted 4 March 2003

ABSTRACT: A novel aromatic amine organo-modifier synthesized in our previous work was used to treat montmorillonite (MMT) and the organo-modified MMT was used to prepare poly(etherimide) (PEI)/MMT nanocomposites by a melt intercalation method. MMT treated by this amine exhibited large layer-to-layer spacing and a high ion-exchange ratio (>95%). The nanocomposites were characterized with X-ray diffraction (XRD), transmission electron microscopy (TEM), dynamic mechanical analysis, a universal tester, thermogravimetric analysis, and by differential scanning calorimetry. The results of XRD and TEM showed that the nanocomposites formed exfoliated structures even when the MMT content was 10 wt %. When the MMT content was below 3 wt %, the PEI/MMT nanocomposites were strengthened and toughened at the same time. The nanocomposites also showed marked decreases in coefficient of thermal expansion and solvent uptake. © 2003 Wiley Periodicals, Inc. J Appl Polym Sci 90: 1857–1863, 2003

Key words: montmorillonite; poly(etherimide); nanocomposites; melt intercalation; thermal properties

INTRODUCTION

The field of polymer/clay nanocomposites or hybrids has recently received considerable attention.[1–25] Since the Toyota Research Center[2,3] first reported on a nylon-6/clay nanocomposite, many polymers have been used to prepare polymer/clay nanocomposites successfully, such as polypropylene,[4–8] polystyrene,[9,10] polyimide,[11–14] epoxy resin,[15,16] polycarbonate,[17] and poly(methyl methacrylate).[18,19] These nanocomposites usually possess improved strength, enhanced modulus, decreased thermal expansion coefficients, increased thermal stability, and reduced gas permeability, compared to the pure polymers or conventional composites, because of the nanoscale dispersion of clay in the polymer matrix, the high aspect ratio of clay platelets, and the strong interfacial interaction between clay and polymers.

Various preparation approaches have been explored to obtain these nanocomposites. The two most commonly used approaches are polymer melt intercalation[6] (in which the nanocomposites are prepared by mixing the clay and the polymer in processing equipment at high temperature and under high shear) and monomer intercalation *in situ* polymerization (in which monomers are intercalated into the clay galleries followed by polymerization).[2,3] Although the monomer intercalation *in situ* polymerization method has been gaining success in the preparation of certain polymer/clay nanocomposite systems, polymer melt intercalation is by far the more popular approach to produce polymer/clay nanocomposites because the whole fabrication process can be fulfilled using conventional polymer-processing techniques. The high temperature and high shear existing in the processing machine may contribute to form an "exfoliation" morphology, which is widely thought to be beneficial to the performance improvement of the composites.[24]

Aromatic polyimide is a type of high-performance polymer with characteristics of a very rigid molecular structure and thermally stable imide units, leading to outstanding mechanical and electrical properties, especially at elevated temperatures. It has been widely applied in aerospace[26] and microelectronic fields.[27] However, the structural characteristics also lead to its poor processability. Commonly used aromatic polyimides are neither soluble nor fusible. They are usually processed in their precursor [poly(amic acid) (PAA)] solution form. An attempt to incorporate clay in polyimide to form nanocomposites was first explored by Yano et al.[14]: they introduced the monomers (pyromellitic dianhydride and 4,4′-diaminodiphenylether) to the dispersion of organically treated montmorillonite, a most widely used 2 : 1 layered structure type of clay, in N-methyl-2-pyrrolidone. The intercalation of the monomers to the clay interlayers followed by polymerization led to a PAA/clay nanocomposite solution, which was further converted to a polyimide/clay nanocomposite by thermal treatment,

Correspondence to: J. Yin (jyin@sjtu.edu.cn).

Contract grant sponsor: Ministry of Education of China.

Contract grant sponsor: Science and Technology Commission of Shanghai Municipal Government; contract grant number: Nano-Project 0214NM019.

Journal of Applied Polymer Science, Vol. 90, 1857–1863 (2003)

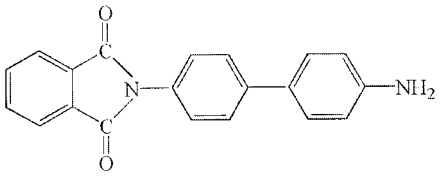

Scheme 1 Chemical structure of OM-*l*.

to remove the solvent and imidize PAA. This monomer intercalation *in situ* polymerization method has been followed by most researchers to prepare polyimide/clay nanocomposites.[11,12] Recently, Huang et al.[24] and Morgan et al.[30] reported on the preparation and the morphological structure of poly(etherimide) (PEI)/MMT nanocomposites, respectively.

PEI resin is a type of amorphous thermoplastic polymer that has interesting physical and chemical properties, making it an attractive candidate for many applications. The ether linkage supplies chain flexibility and good melt flow characteristics, whereas the imide units provide thermal resistance and mechanical properties. Although PEI has good melt processability, its relatively poor solvent resistance, size stability (high coefficient of thermal expansion), and thermal stability limit its application in aerospace and microelectronics. In this report, we continue our study on PEI/MMT nanocomposites by investigating the mechanical, thermal properties, size stability, and solvent resistance. We used a thermally stable aromatic amine to pretreat MMT. The amine contains the thermally stable phenyl structure and imide moiety and, unlike aliphatic amines, has a very rigid chemical structure (Scheme 1). The treated MMT may possess better compatibility with PEI because of the structural similarity between the treatment agent and PEI.

EXPERIMENTAL

Materials

Sodium montmorillonite (Na-MMT) with a cation exchange capacity (CEC) of 100 meq/100 g was supplied by the Institute of Chemical Metallurgy, Chinese Academy of Sciences. The average particle size was 50 μm. *N*-[4-(4′-Aminophenyl)]phenyl phthalimide (OM-*l*) was synthesized in our lab.[21] The thermoplastic PEI was provided by the Shanghai Research Institute of Synthetic Resin, whose chemical structure is shown in Scheme 2. Other common reagents such as ethanol and xylene were purchased from Shanghai Reagent Company and used without further purification.

Preparation of organically modified MMT (MMT-*l*)

MMT was organically modified with OM-*l* by an ion-exchange reaction in water. The mixture of 10.8 g OM-*l*, 1 mL concentrated hydrochloric acid (37%), and 150 mL distilled water was heated at 80°C, and to this mixture was added a dispersion of 25 g Na-MMT in 1000 mL distilled water. The mixture was stirred vigorously for 1 h at 80°C. The white precipitate was filtered and washed repeatedly with hot water (80°C), to remove both the superfluous ammonium salts and the Cl^-, and was subsequently collected and dried in vacuum at 80°C for 24 h.

Preparation of PEI/MMT nanocomposites

PEI and MMT-*l* were dried at 120 and 40°C for 2 h, respectively, in vacuum before use. PEI and various amounts of MMT-*l* were dry-mixed and melt-blended at 370°C for 30 min by using the internal mixer of a Haake Rheocord System. The mixture was pressed in a hot press at 370°C and then in a cold press at room temperature, and PEI/MMT nanocomposite films of about 0.2 mm thickness were obtained.

Characterization

The wide-angle X-ray diffraction patterns of MMT and PEI/MMT composites were recorded on a Rigaku (Japan) Geiger Flex D/max-RB diffractometer using Cu–K_α radiation (40 kV, 100 mA, λ = 0.154 nm) filtered by Cr in a range of 2θ = 1.0–35° with a scan rate of 4°/min. The basal interlayer spacing of MMT was estimated from the position of the (001) plane peak in the X-ray diffraction (XRD) intensity profile using Bragg's equation, $d = \lambda/2 \sin \theta_{max}$. Samples for transmission electron microscopic (TEM) analysis were prepared by placing small strips of sample films in epoxy resin and then cut using an ultratome and placed on a 200-mesh copper grid for analysis. The TEM investigations were performed on a JEM-100CXII TEM operating at an acceleration voltage of 100 kV.

The glass-transition temperatures (T_g's) were determined by differential scanning calorimetric (DSC) curves, which were measured on a Perkin–Elmer Pyris I DSC (Perkin Elmer Cetus Instruments, Norwalk, CT)

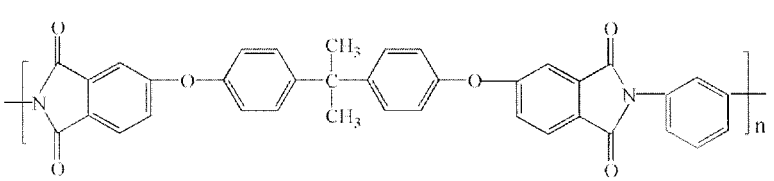

Scheme 2 Chemical structure of PEI.

under the protection of N_2 at a heating rate of 20°C/min. The thermal stability of PEI/MMT nanocomposites was determined by thermal gravimetric analysis, which was conducted on a Perkin–Elmer TGA 7 under N_2 flow. The temperature range was 100 to 800°C with a heating rate of 20°C/min. The dynamic thermal analysis (DMA) of the PEI and PEI/MMT nanocomposite films was conducted on a TA 2980 DMA (TA Instruments, New Castle, DE) at a heating rate of 5°C/min. The coefficient of thermal expansion (CTE) of the PEI and the PEI/MMT nanocomposite films was also measured on a TA 2980 DMA with a TMA mode. The film was pretreated at 150°C for 20 min to eliminate the internal stress. The load on the film was 100 mN and the heating rate was 5°C/min. A temperature range of 60–150°C was selected to calculate the CTE.

The stress–strain curves of PEI and PEI/MMT nanocomposite films were recorded on an Instron-4465 Universal Tester (Instron, Canton, MA) at room temperature at a drawing rate of 5 mm/min. The sorption experiments were carried out by the following procedure. The sample films were dried in an oven at 105°C for 8 h, then kept in the solvents at different temperatures for a given period of time, and blotted to remove the excessive solvent. The amount of absorbed solvent was calculated from the increase in the weight of the samples.

RESULTS AND DISCUSSION

Organo-modification of MMT

The organo-modification of MMT is an important step in the preparation of polymer/MMT nanocomposites and the quaternary ammonium salts of primary aliphatic amines such as 1-hexadecylamine have been commonly used as such organic modifiers. It has been accepted that the polar cationic head group of the modifier molecule would preferentially reside at the polar layer surface and the nonpolar aliphatic tail would radiate away from the surface of clay layers.[22] Quaternary ammonium salts could undergo an ion-exchange reaction with inorganic cations in the galleries of MMT to lead to a more hydrophobic MMT. The long aliphatic groups could also increase the MMT layer-to-layer spacing. The result of these two changes facilitates the intercalation of polymer or monomer molecules into interlayers of MMT. In this study, we used an aromatic amine (OM-*l*) as the modifier. Figure 1 shows the XRD patterns of Na-MMT, MMT-*l*, and PEI/MMT nanocomposites. Table I lists the basal spacing of Na-MMT and MMT-*l* calculated from Bragg's equation. The interlayer spacing of MMT was obviously increased after the treatment with chloride salt of OM-*l* from $d = 1.24$ nm for pure Na-MMT to $d = 2.90$ nm for MMT-*l*. It was found that this basal spacing of MMT-*l* was greater than that for MMT treated by the commonly used 1-hexadecylamine.[23] Measurement by inductively coupled plasma (emission spectroscopy) also revealed a very high ion-exchange ratio in the OM-*l*–treated MMT (Table I). All these results suggested that OM-*l* was very effective in modifying MMT.

TABLE I
***d*-Value of MMT Modified with OM-*l* and Mean Value of Percentage Recovery of Sodium Ions Measured by ICP**

Sample	2θ (°)	*d* (nm)	Sodium ions (wt %)	Ion exchange ratio
Na–MMT	7.12	1.24	2.3860	—
MMT–*l*	3.04	2.90	0.0417	98.25
	6.30	002 Peak		

Dispersion of MMT in PEI matrix

The diffraction peaks of MMT were not observed in XRD patterns of PEI/MMT nanocomposites up to 10 wt % MMT content (Fig. 1), probably indicating that layered MMT was exfoliated. The "exfoliation morphology" of the PEI/MMT nanocomposites was also confirmed by TEM analysis (Fig. 2). In the TEM pho-

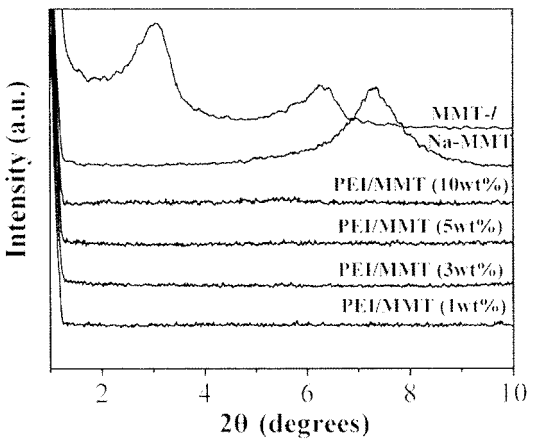

Figure 1 XRD patterns of Na-MMT, MMT-*l*, and PEI/MMT nanocomposites.

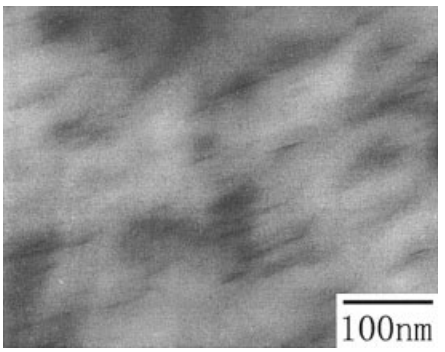

Figure 2 TEM photograph of PEI/MMT nanocomposite containing 5 wt % MMT

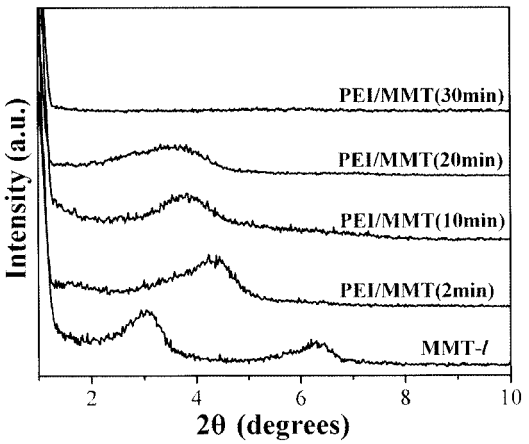

Figure 3 XRD patterns of MMT-*l* and PEI/MMT nanocomposites.

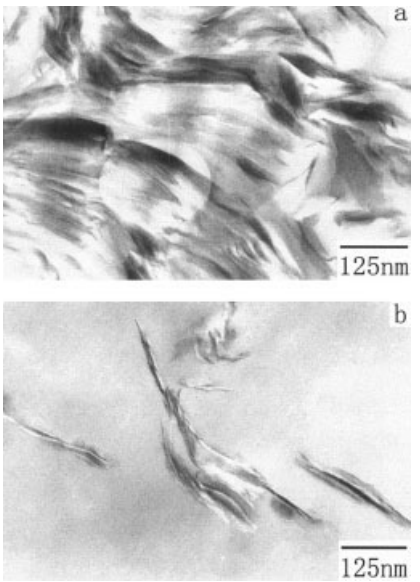

Figure 4 TEM photographs of PEI/MMT nanocomposite containing 5 wt % MMT at different blending times: (a) 2 min; (b) 10 min.

tographs, the dark lines represent the intersections of MMT layers, whereas the gray areas represent the PEI matrix. It was observed that the MMT layers were dissociated and dispersed homogeneously in the PEI matrix. In our previous studies,[23] we prepared a series of PI/MMT nanocomposites containing various amounts of MMT using the monomer intercalation *in situ* polymerization procedure at room temperature, in which only "intercalation morphology" could be achieved when the MMT content was higher than 3 wt %. The formation of the "exfoliation morphology" in this study may be attributed to the high temperature and strong shear field in the internal mixer, the high viscosity of molten PEI, and the strong interactions between MMT and PEI. Figure 3 shows the XRD patterns of PEI/MMT nanocomposites containing 5 wt % MMT blended for different periods of time. With increasing blending time, the diffraction peak of MMT-*l* shifted gradually to a lower angle, indicating increased layer-to-layer spacing. The diffraction intensity also weakened gradually and finally completely disappeared. The change in the morphological structure of the composites can be further clearly studied by TEM analysis. Figure 4(a,b) shows TEM photographs of the PEI/MMT nanocomposites containing 5 wt % MMT blended for 2 and 10 min in the internal mixer. When MMT and PEI were blended for 2 min [Fig. 4(a)], the face-to-face associated MMT layers were dominant. When they were blended for 10 min [Fig. 4(b)], the spacing of the silicate layers increased to 6–7 nm and the face-to-face associated layers were oriented in the shear field and slipped in a staircase-like fashion. As the blending time was further increased to 30 min (Fig. 2), the MMT layers were completely dissociated. Thus it is clear that the intercalation capability of the polymer and the strong shear field played important roles in the preparation of exfoliated polymer/MMT nanocomposites by the melt intercalation method.

Mechanical properties of PEI/MMT nanocomposites

Figure 5 shows the relationship between MMT content and the Young's modulus of the PEI/MMT nanocomposite films: the modulus increased with the MMT content, reaching a maximum at 3 wt %. This increase in modulus may be caused by the strong interaction between the MMT layers and PEI, and the MMT sheets acted as "crosslinking point," which limited the PEI chain movement. When the MMT content was further increased, the Young's modulus of the nanocomposite films decreased drastically. Because an "exfoliation morphology was still obtained at a MMT content greater than 3 wt %, this decrease in the Young's modulus could not be attributed to the change in morphological structure. Gilman and coworkers[28,29] studied the number-average molecular

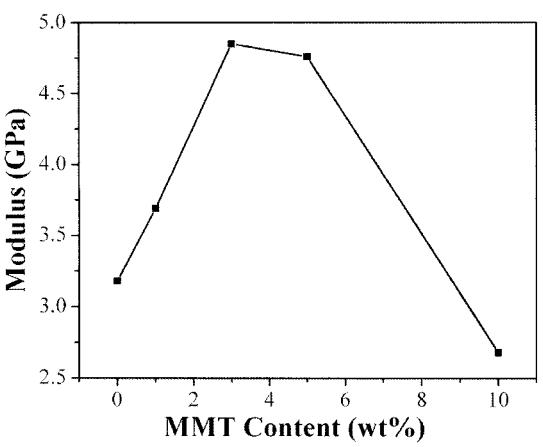

Figure 5 Young's modulus of the PEI/MMT nanocomposites.

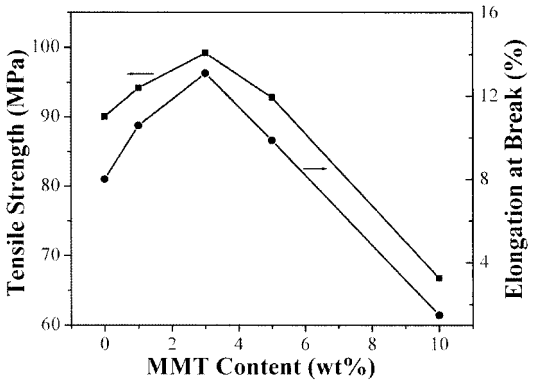

Figure 6 Tensile strength and elongation at break of PEI and PEI/MMT nanocomposites.

weight (M_n) of PS/MMT nanocomposites and found that the presence of the quaternary alkylammonium in the MMT somehow contributed to the degradation of PS. The decrease in M_n had a direct negative impact on the flame-retardant performance by reducing the melt viscosity and could also limit the improvements in other physical properties observed for PS/MMT nanocomposites. For PEI/MMT nanocomposites, the concentration of organo-modifier was increased when the MMT content was increased, which might cause degradation of PEI and the decrease in Young's modulus.

The tensile strength and the elongation at break of PEI and PEI/MMT nanocomposite films with various MMT contents are shown in Figure 6. When the MMT content was less than 3 wt %, both the tensile strength and the elongation at break of PEI/MMT films were increased with the increase of MMT content. The tensile strength was increased from 90.06 MPa for PEI to 99.21 MPa for PEI/MMT (a 10.2% increase), whereas the elongation at break was increased from 8.0% for PEI to 13.1% for PEI/MMT (a 63.8% increase) nanocomposites containing 3 wt % MMT. Combining the foregoing results, when the MMT content was below 3 wt %, with the help of the strong shear field, an exfoliated dispersion of MMT in PEI could be obtained, indicating that PEI could be strengthened and toughened simultaneously by the introduction of exfoliated MMT. The strong interfacial interaction between PEI and MMT, and the existence of the large shear zone, increased the tensile strength of the nanocomposite. Moreover, the large amount of interface between the exfoliated MMT sheets and PEI could effectively and simultaneously reduce the formation of the shear zone to cracks. When the MMT content exceeded 3 wt %, both the tensile strength and the elongation at break were decreased, probably for the same reason as for the Young's modulus.

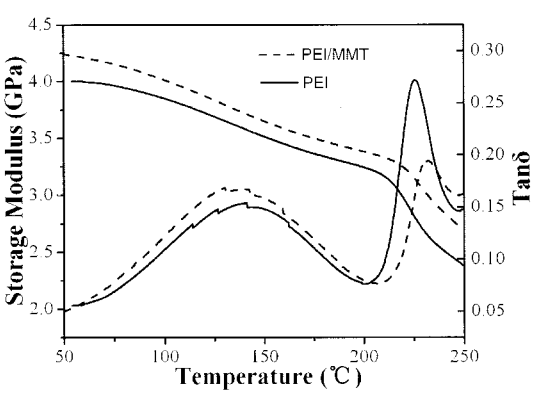

Figure 7 DMA curves of PEI and PEI/MMT nanocomposites containing 3 wt % MMT.

TABLE II
Dynamic Storage Modulus of PEI and PEI/MMT Nanocomposites Containing 3 wt % MMT and Their Glass-Transition Temperatures Obtained from tan δ

Sample	Storage modulus (Gpa)				Glass-transition temperature[a] (C)
	60	120	180	240	
PEI	3.99	3.71	3.33	2.47	224.8
PEI/MMT	4.22	3.86	3.46	2.79	230.0

[a] The glass-transition temperatures were measured at the peak tops of tan δ.

Figure 7 shows the DMA curves of the PEI and PEI/MMT nanocomposite films containing 3 wt % MMT. The tan δ peak of PEI/MMT nanocomposites gradually shifted to a slightly higher temperature and broadened in comparison to PEI. This could be also explained by the existence of a strong interaction between MMT and the PEI matrix, which limited the movement of PEI chain segments. Table II shows the dynamic storage moduli of PEI and PEI/MMT nanocomposite films containing 3 wt % MMT at various temperatures and their glass-transition temperatures obtained from tan δ. It was found that the storage modulus of PEI below and above its T_g was increased when a small amount of MMT was introduced.

TABLE III
Onset Thermal Decomposition Temperature and 5 and 10% Weight Loss Temperatures of PEI and PEI/MMT Nanocomposites

Temperature parameter	MMT content (wt %)				
	0	1	3	5	10
T_d(°C)[a]	522	526	527	531	534
T_5(°C)[b]	520	524	525	526	528
T_{10}(°C)[c]	542	543	546	548	550
T_g(°C)[d]	207	208	209	205	199

[a] Thermal decomposition temperature (onset) from TGA measurement. Scan rate: 20°C/min, N_2 protection.
[b] Temperature at 5% weight loss from TGA measurement. Scan rate: 20°C/min, N_2 protection.
[c] Temperature at 10% weight loss from TGA measurement. Scan rate: 20°C/min, N_2 protection.
[d] Glass-transition temperature obtained from DSC measurements. Scan rate: 20°C/min, N_2 protection.

Thermal properties of PEI/MMT nanocomposites

The data of Table III show the onset thermal decomposition temperatures, and the temperatures for 5 and 10% weight loss of PEI and PEI/MMT nanocomposites determined by TGA. They were slightly increased with the increase of MMT content. The onset thermal decomposition temperature was increased from 522°C for PEI to 534°C for PEI/MMT nanocomposite containing 10 wt % MMT. MMT possessed higher thermal stability and its layer structure exhibited a greater barrier effect to hinder the evaporation of the small molecules generated in the thermal decomposition to limit the continuous decomposition of the PEI matrix.

Figure 8 shows DSC traces of PEI and PEI/MMT nanocomposites with various MMT contents. For MMT content below 3 wt %, the T_g of the nanocomposites was slightly increased as the MMT content was increased: the T_g was increased from 207°C for PEI to 209°C for the nanocomposite containing 3 wt % MMT. When the MMT content was greater than 3 wt %, the T_g of the nanocomposites was slightly decreased as the MMT content was increased. At the 370°C processing temperature, the organo-modifier decomposed and was released from the nanocomposites, although some small organic molecules might still have been trapped in the PEI matrix. With increased MMT contents, the existence of more organic molecules may lead to plasticization and thus to the slight decrease in T_g of the nanocomposites.

The reduced segmental movement of the PEI matrix by the introduction of "exfoliated" MMT sheets would also lead to a decrease in the CTE. Figure 9 represents the relationship between the MMT content and the CTE of the PEI/MMT nanocomposite films. The CTE decreased from 2.37×10^{-5} K^{-1} for PEI to 1.33×10^{-5} K^{-1} (a 44% decrease) for PEI/MMT nanocomposite containing 10 wt % MMT. The decrease in CTE (or increase in size-stability) is extremely desirable when PEI is applied in microelectronic and optoelectronic fields.

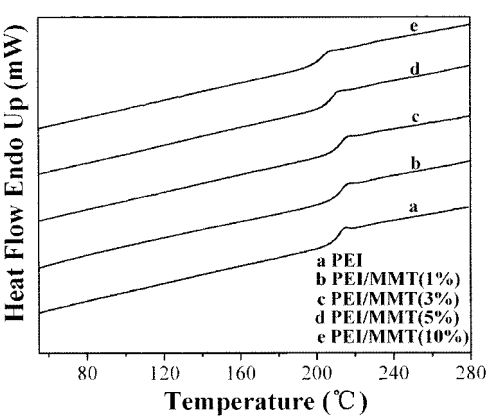

Figure 8 DSC curves of PEI and PEI/MMT nanocomposites.

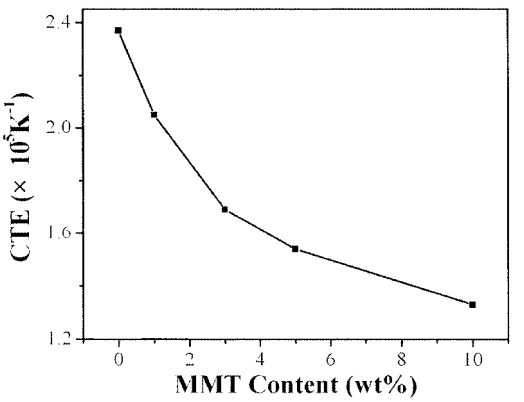

Figure 9 Coefficient of thermal expansion of PEI/MMT nanocomposites.

Solvent resistance of PEI/MMT nanocomposites

Table IV lists the results of solvent-uptake measurements of PEI and PEI/MMT nanocomposites with various MMT contents. First, the samples were immersed in solvents at 25°C for 24 h, although it was observed that the solvent uptake had not reached equilibrium. So, the samples were immersed for another 2 days, and heated to 100°C for 1 h, with the aim of investigating the solvent resistance at a relatively high temperature and the saturated solvent uptake of the PEI/MMT nanocomposites. It was observed that the introduction of MMT led to an obvious decrease in the solvent uptake in both processes. For example, the water-uptake ratios decreased, from 0.90% (25°C) and 1.29% (100°C) for PEI, to 0.38% (25°C) and 0.54% (100°C) for PEI/MMT nanocomposites containing 10 wt % MMT. The decrease in solvent uptake of the PEI/MMT nanocomposites may be attributed to the following reasons. First, the strong interaction between MMT and PEI matrix led to the formation of "bound polymer," polymer in close proximity to the reinforcing filler (MMT), which was either physisorbed or chemisorbed and therefore restricted the solvent uptake.[25] Second, the large aspect ratio of MMT layers possessed excellent barrier properties, and the exfoliated structure of MMT layers especially could maximize the available surface area of the reinforcing phase. The reduction in water uptake is extremely desirable when PEI is to be applied in microelectronic fields because high water uptake of polymers used in microelectronic devices (polyimide and epoxy) is one of the major causes affecting their long-term stability.

CONCLUSIONS

PEI/MMT nanocomposites were successfully prepared by the melt intercalation approach. From XRD and TEM results, the MMT layers were basically exfoliated in the nanocomposites even when the MMT content was 10 wt %. The MMT content significantly

TABLE IV
Solvent Uptake Ratios of PEI and PEI/MMT Nanocomposites

Solvent uptake ratio (%)[a]	Water		Ethanol		Xylene	
	25°C[b]	100°C[c]	25°C	100°C	25°C	100°C
PEI	0.90	1.29	0.52	0.56	0.78	1.52
PEI/MMT-1%	0.83	0.95	0.08	0.21	0.72	1.32
PEI/MMT-3%	0.71	0.87	0.06	0.20	0.49	1.08
PEI/MMT-5%	0.55	0.77	0	0.18	0.42	0.90
PEI/MMT-10%	0.38	0.54	0	0.03	0.28	0.50

[a] The calculation formula of the solvent uptake ratio: $(W_{wet} - W_{dry})/W_{dry} \times 100\%$.
[b] The sample was soaked in solvent at 25°C for 24 h.
[c] The sample was soaked in solvent at 25°C for 3 days, 100°C for 1 h.

influenced the properties of PI/MMT nanocomposites. When the MMT content was below 3 wt %, the PI/MMT nanocomposites were strengthened and toughened at the same time. The introduction of MMT also led to improvement in thermal stability and marked decreases in coefficient of thermal expansion and solvent uptake. Overall, the nanocomposites possessed excellent mechanical and thermal properties when the MMT content was 3 wt %.

The authors thank the Ministry of Education of China (Kuashiji Scholars' Project) and the Science and Technology Commission of Shanghai Municipal Government (Nano-Project 0214NM019) for their financial support.

References

1. Giannelis, E. P.; Krishnamoorti, R.; Manias, E. Adv Polym Sci 1999, 138, 107.
2. Kojima, Y.; Usuki, A.; Kawasumi, M.; Okada, A.; Kurauchi, T.; Kamigaito, O. J Polym Sci Part A: Polym Chem 1993, 31, 983.
3. Kojima, Y.; Usuki, A.; Kawasumi, M.; Okada, A.; Kurauchi, T.; Kamigaito, O. J Polym Sci Part A: Polym Chem 1993, 31, 1755.
4. Hasegawa, N.; Kawasumi, M.; Kato, M.; Usuki, A.; Okada, A. J Appl Polym Sci 1998, 67, 87.
5. Kurokawa, Y.; Yasuda, H.; Oya, A. J Mater Sci Lett 1996, 15, 1481.
6. Kawasumi, M.; Hasegawa, N.; Kato, M.; Usuki, A.; Okada, A. Macromolecules 1997, 30, 6333.
7. Zhang, Q.; Fu, Q.; Jiang, L. X.; Lei, Y. Polym Int 2000, 49, 1561.
8. Sun, T.; Garces, J. M. Adv Mater 2002, 14, 128.
9. Doh, J. G.; Cho, I. Polym Bull 1998, 41, 511.
10. Zhu, J.; Morgan, A. B.; Lamelas, F. J.; Wilkie, C. A. Chem Mater 2001, 13, 3774.
11. Agag, T.; Koga, T.; Takeichi, T. Polymer 2001, 42, 3399.
12. Chang, J. H.; Park, K. M. Polym Eng Sci 2001, 41, 2226.
13. Chin, I. J.; Thurn-Albrecht, T.; Kim, H. C.; Russell, T. P.; Wang, J. Polymer 2001, 42, 5947.
14. Yano, K.; Usuki, A.; Okada, A.; Kurauchi, T.; Kamigaito, O. J Polym Sci Part A: Polym Chem 1993, 31, 2493.
15. Yano, K.; Usuki, A.; Okada, A. J Polym Sci Part A: Polym Chem 1997, 35, 2289.
16. Salahuddin, N.; Moet, A.; Hiltner, A.; Baer, E. Eur Polym J 2002, 38, 1477.
17. Huang, X. Y.; Lewis, S.; Brittain, W. J. Macromolecules 2000, 33, 2000.
18. Lee, D. C.; Jang, L. W. J Appl Polym Sci 1996, 61, 1117.
19. Chen, H.; Yao, K.; Tai, J. J Appl Polym Sci 1999, 73, 425.
20. Delozier, D. M.; Orwoll, R. A.; Cahoon, J. F.; Johnston, N. J.; Smith, J. G., Jr.; Connell, J. W. Polymer 2002, 43, 813.
21. Yang, Y.; Zhu, Z.; Yin, J.; Wang, X.; Qi, Z. Polymer 1999, 40, 4407.
22. Vaia, R. A.; Teukolsky, R. K.; Giannelis, E. P. Chem Mater 1994, 6, 1017.
23. Liang, Z. M.; Yin, J.; Xu, H. J. Polymer 2003, 44, 1391.
24. Huang, J. C.; Zhu, Z. K.; Yin, J.; Qian, X. F.; Sun, Y. Y. Polymer 2001, 42, 873.
25. Kraus, G. J. J Appl Polym Sci 1963, 7, 861.
26. Xie, W.; Pan, W.-P.; Chuang, K. C. Thermochim Acta 2001, 367–368, 143.
27. Yu, J.; Ree, M.; Shin, T. J.; Wang, X.; Cai, W.; Zhou, D.; Lee, K.-W. Polymer 2000, 41, 169.
28. Gilman, J. W.; Jackson, C. L.; Morgan, A. B.; Harris, R. H.; Manias, E.; Giannelis, E. P.; Wuthenow, M.; Hilton, D.; Phillips, S. Chem Mater 2000, 12, 1866.
29. Gilman, J. W.; Awad, W. H.; Davis, R. D.; Shields, J.; Harris, R. H., Jr.; Davis, C.; Morgan, A. B.; Sutto, T. E.; Callahan, J.; Trulove, P. C.; Delong, H. C. Chem Mater 2002, 14, 3776.
30. Morgan, A. B.; Gilman, J. W.; Jackson, C. L. Macromolecules 2001, 34, 2735.